8th GRACM International Congress on Computational Mechanics,
Volos, 12 July - 15 July 2015

Stick-slip motion and hysteresis behaviour of droplets with dynamic volume variation

Marc Pradas[1], Nikos Savva[2], Jay B. Benziger[3], Ioannis G. Kevrekidis[3] & Serafim Kalliadasis[4]

[1]Department of Mathematics and Statistics, The Open University, Milton Keynes MK7 6AA, UK
[2]School of Mathematics, Cardiff University, Cardiff CF24 4AG, UK
[3]Department of Chemical and Biological Engineering, Princeton University, Princeton NJ 08544, USA
[4]Department of Chemical Engineering, Imperial College London, London SW7 2AZ, UK

Keywords: Contact line dynamics, fluid transport, diffuse interface modelling.

Abstract: *We investigate the dynamics of a droplet on a planar substrate as its volume increases or decreases. We adopt a diffuse-interface model that incorporates an inflow/outflow boundary condition at the bottom-center of the droplet, hence allowing to dynamically control its volume, and we consider a topographically smooth substrate with a periodic chemical pattern. We observe that the droplet undergoes a stick-slip motion as the volume is increased (inflow conditions) which can be monitored by e.g. looking at the contact points. When we switch over to outflow conditions the droplet follows a different path giving rise to a hysteresis behaviour.*

1 INTRODUCTION

The process of a droplet spreading over complex geometries is found in many different applications, from microchemical reactors and fluid transport processes to material processing and digital microfluidic systems, to name but a few. In most cases substrates are not smooth but are charactarised by various complexities such as chemical and/or topographical variations which give rise to a very rich dynamics characterised by e.g. hysteresis behaviour [20, 21, 22]. Examples of complex substrates include the case of a membrane or a porous medium where in addition to the intrinsic properties of the material one needs to take into account the fact that the volume of the droplet may vary in time, i.e. liquid can be absorbed or pumped in through the membrane [2], something common in e.g. polymer electrolyte membrane (PEM) fuel cells [7, 11, 6]. In these particular systems, water is formed at a catalyst/membrane interface and is pushed through porous electrodes into a gas flow channel. It is observed that water drops emerge from the largest pores in the electrode and grow in the main channel (i.e. drops experience a dynamic volume variation). These droplets must then detach and be pushed through the gas flow channel in contact with the electrode porous surface: they need to be removed from the device to avoid issues such as flooding. Hence, it is important to note that once the droplets are created and are growing into the main channel, they are constantly in contact with a disordered substrate (i.e. the electrode membrane) which may affect the whole process.

In addition to PEM fuel cells, droplets with a time-dependent volume are found in many other applications, such as for example in microemulsification, and systems with non-equilibrium thermal effects such as evaporation [16]. Understanding the interplay between dynamic volume variation and other parameters of the system (e.g. the substrate chemical properties) is of crucial importance in a wide spectrum of technological applications including the rapidly growing fields of micro- and nanofluidics; and while this problem has received some attention over the last few decades, both experimentally [9, 12] and analytically [17, 10, 3], it is still unclear how the dynamics of the droplet itself, as its volume increases or decreases in time, is affected by the properties of the solid susbtrate.

Here we investigate a simple prototype system, a two-dimensional (2D) droplet sitting on a substrate with a small pore from which liquid can be either pumped in or out. To this end, we adopt a diffuse-interface Cahn-Hilliard model (see [19, 26]) that incorporates an extra boundary condition (BC) from which we can impose either a positive (inflow) or negative (outflow) constant liquid flow into the droplet, hence allowing to dynamically control its volume. As for the solid substrate, we consider a topographically smooth substrate with a periodic chemical pattern, i.e. the equilibrium contact angle varies periodically along the substrate. Under these conditions, we observe that the droplet exhibits a stick-slip dynamics as the volume is increased (inflow conditions) which we monitor by looking at the displacement of the droplet. When we switch over to outflow conditions (i.e. the volume

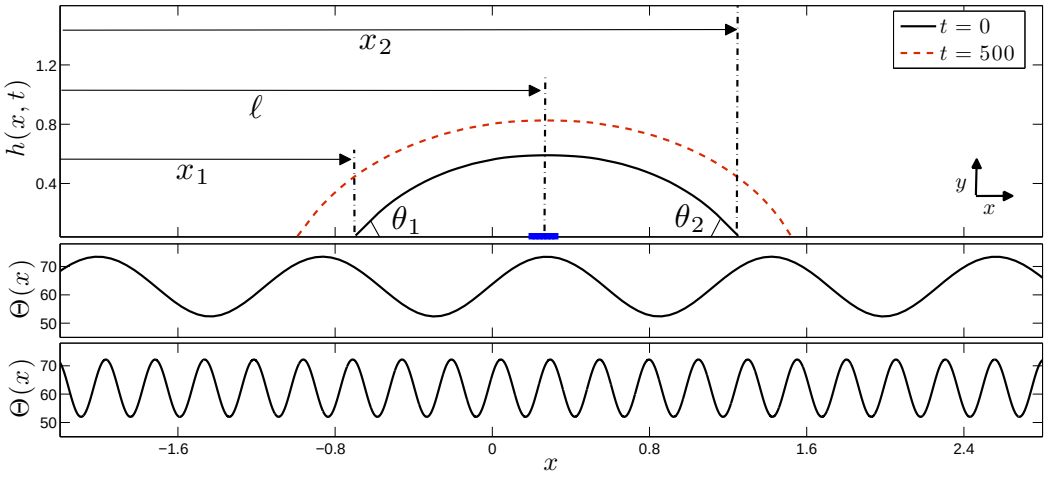

Figure 1: Numerical computations of a droplet with an inflow BC obtained at two different times. The location of the small pore is marked as a blue rectangle. The points x_1 and x_2 correspond to the contact points, ℓ corresponds to the displacement of the droplet, and θ_1 and θ_2 the contact angles. The bottom panels show the periodic variation of the chemical substrate which is prescribed by the function $\Theta(x)$, for $\lambda = 20$ (middle panel) and $\lambda = 100$ (bottom panel), and represents the imposed contact angle, given in degrees.

decreases) the droplet exhibits again stick-slip motion but it now follows a different path giving rise to a hysteresis behaviour. Hence, a simple chemical heterogeneous substrate is able to induce a complex behaviour in the droplet dynamics.

The manuscript is organised as follows. Section 2 sets up the problem and introduces the computational framework. Section 3 outlines the different results of our study, and we conclude in Sec. 4.

2 PROBLEM FORMULATION

The system setup consists of a 2D droplet on top of a flat substrate which has been chemically altered so that its wetting properties (i.e. the contact angle, which is defined as the angle between the liquid-gas interface and the wetted area of the substrate) vary periodically along the substrate. In particular, we consider an oscillatory variation of the equilibrium contact angle which is prescribed by the function:

$$\Theta(x) = \theta_0 + \sigma \sin(\lambda x), \tag{1}$$

where θ_0 is the equilibrium contact angle for the homogeneous substrate, and σ and λ represent the intensity and wavelenght of the disorder variation, respectively. We are interested in studying the dynamic properties of the droplet as its volume is increased or decreased and so we impose a BC on the susbtrate through which liquid can be pumped in or out. To monitor the droplet dynamics we then look at different dynamic quantities describing the droplet as the volume $V(t)$ varies in time, namely the displacement of the droplet, ℓ, which is obtained through the two contact points of the droplet (say x_1 and x_2 for left and right contact point, respectively) as $\ell(t) = (x_1(t) + x_2(t))/2$, the droplet base $d(t) = (x_2(t) - x_1(t))/2$, and the contact angles $\theta_1(t)$ and $\theta_2(t)$ (see Fig. 1).

2.1 Diffuse interface modelling

To model our system we make use of a Cahn-Hilliard phase-field formulation which is generally used to describe a system of two phases separated by a diffuse interface (see e.g. [1, 27]). In this approach, a locally conserved field, denoted as ϕ, plays the role of an order parameter by taking two equilibrium limiting values $+\phi_e$ and $-\phi_e$ that represent the liquid and air phases, respectively. The interface position of the droplet, which we denote as $h(x,t)$, is then located at the points where the order parameter vanishes, i.e., in a 2D system we write $\phi[x, h(x,t)] = 0$. The equilibrium properties of the model are based on a Ginzburg-Landau formulation, where the total free energy of the system is given by

$$\mathfrak{F}(\phi) = \int_\Omega d\mathbf{r}\, f(\phi) = \int_\Omega d\mathbf{r} \left[V(\phi) + \frac{\varepsilon^2}{2} |\boldsymbol{\nabla}\phi|^2 \right], \tag{2}$$

where $f(\phi)$ is the free energy density, Ω corresponds to the system domain, and the potential $V(\phi)$ is usually chosen as:

$$V(\phi) = -\frac{1}{2}\alpha\phi^2 + \frac{1}{4}\beta\phi^4, \tag{3}$$

with α and β being positive constants in such a way that the equilibrium value for the phase field is given by $\phi_e = \sqrt{\alpha/\beta}$. The double-well form of the potential combined with the square gradient term of the free energy ensures the existence of a well-defined interface with a width $\zeta = \varepsilon/\sqrt{\alpha}$. In this formulation, the chemical potential is defined as $\mu = \delta\mathfrak{F}/\delta\phi = V'(\phi) - \varepsilon^2\nabla^2\phi$, and the surface tension of the liquid-gas interface σ_{lg} can be easily obtained as the excess free energy per unit surface area due to the inhomogeneity in ϕ, which gives $\sigma_{lg} = \frac{2\sqrt{2}}{3}\zeta\alpha\phi_e^2$ [4, 26].

To take into account the wetting properties of the solid subtrate, the free-energy equation (2) is modified by adding an extra term associated with solid-fluid interactions [5]

$$\mathfrak{F}(\phi) = \int_\Omega d\mathbf{r}\left[V(\phi) + \frac{\varepsilon^2}{2}|\boldsymbol{\nabla}\phi|^2\right] + \int_s d\mathbf{s} f_s(\phi_s), \tag{4}$$

where s denotes the solid surface. The function $f_s(\phi_s)$ in this additional term which enables us to introduce wetting effects into the model is related to the molecular interactions between fluid and solid, and it is usually expanded as a power series in ϕ_s [8], where ϕ_s represents the value of the phase field at the solid wall. In the present study we shall keep only the first order term and write: $f_s = -a\phi_s$, where a describes the preference of the wall for either the liquid phase ($a > 0$, hydrophilic conditions) or the air phase ($a < 0$, hydrophobic conditions). It is important to emphasize that the linear term in the expansion of f_s turns out to be enough to describe partial wetting situations [23, 4] as the ones we are going to consider here. Note, however, that for situations closer to complete wetting (i.e. contact angles close to zero) higher order terms might need to be included in order to avoid effects induced by the formation of mesoscopic layers on the walls [15, 24, 25].

Our system is non-dimensionalised by choosing the following dimensionless variables:

$$\phi^* = \phi/\phi_e, \qquad \mathbf{r}^* = \mathbf{r}/R_0, \tag{5a}$$

$$f^* = f/(\phi_e^2\alpha), \qquad f_s^* = f_s/\sigma_{lg}, \tag{5b}$$

where R_0 is the initial radius of the droplet. By minimizing the corresponding dimensionless free energy functional, the equilibrium conditions are given as $\mu = \delta\mathfrak{F}/\delta\phi = 0$ and the wetting boundary condition [4, 5]:

$$\mathbf{n_y}\cdot\boldsymbol{\nabla}\phi|_s = \frac{\gamma}{C_n}\frac{df_s}{d\phi_s} = -\frac{\gamma}{C_n}a, \tag{6}$$

where the asterisks have been dropped and we have defined the Cahn number as $C_n = \zeta/R_0$, and $\gamma = 2\sqrt{2}\phi_e/3\sigma_{lg}$. Here, $\mathbf{n_y}$ is the unitary outward normal vector to the wall. For a constant value of a, the corresponding static equilibrium contact angle, θ_e, can be obtained by making use of the Young-Dupré relation, $\cos\theta_e = (\sigma_{sg} - \sigma_{sl})/\sigma_{lg}$, where σ_{sg} and σ_{sl} are the solid-gas and solid-liquid surface tensions, respectively, giving rise to the following relation [5, 4, 14, 18]:

$$\cos\theta_e = \frac{1}{2}\left[(1+A)^{3/2} - (1-A)^{3/2}\right], \tag{7}$$

where we have defined $A = \sqrt{2}\gamma a$. In this approach, the different surface tensions σ_{sg} and σ_{sl} can be obtained by integrating the free energy per unit area along the corresponding interfaces, solid-gas and solid-liquid [4].

Finally, the dynamics of the phase field is assumed to follow a conserved equation based on a time-dependent Ginzburg-Landau Hamiltonian (model B in the Hohenberg and Halperin nomenclature [13]). In a quasistatic limit it reads in dimensional form as:

$$\frac{\partial\phi}{\partial t} = \boldsymbol{\nabla}\cdot M\boldsymbol{\nabla}\mu = \boldsymbol{\nabla}\cdot M\boldsymbol{\nabla}\left(-\alpha\phi + \beta\phi^3 - \varepsilon^2\nabla^2\phi\right), \tag{8}$$

where μ is the chemical potential defined earlier, and M is a mobility parameter which we take to be $M = 1$. To implement an inflow/outflow BC at a single pore of length ℓ_p which is located within the region where the droplet is lying on, we impose a constant gradient of chemical potential along ℓ_p. In particular, we take

$$\mathbf{n_y}\cdot\boldsymbol{\nabla}\mu|_{\{x\in[\ell_0-\ell_p/2,\ell_0+\ell_p/2],y=0\}} = -v_m, \tag{9}$$

where ℓ_0 is the initial value of the droplet displacement, and v_m is a constant parameter that controls the flow that is being pumped in ($v_m > 0$) or out ($v_m < 0$).

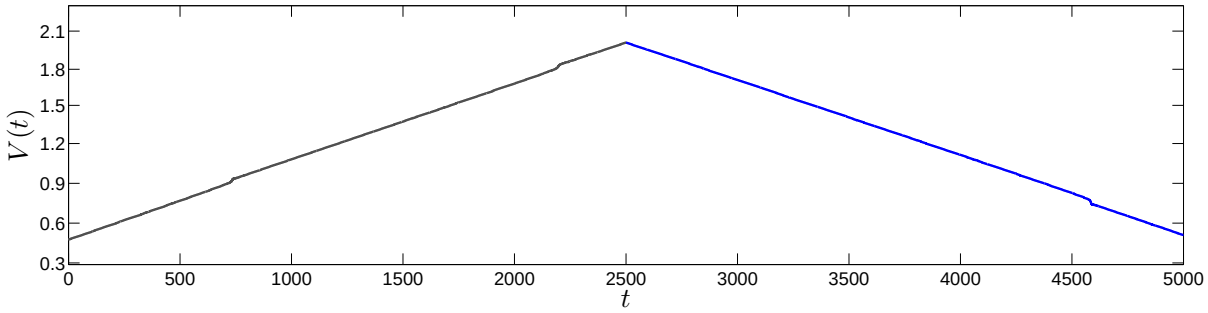

Figure 2: Time-dependent volume for inflow conditions (up to $t = t_f = 2500$) and outflow conditions (for $t > t_f$).

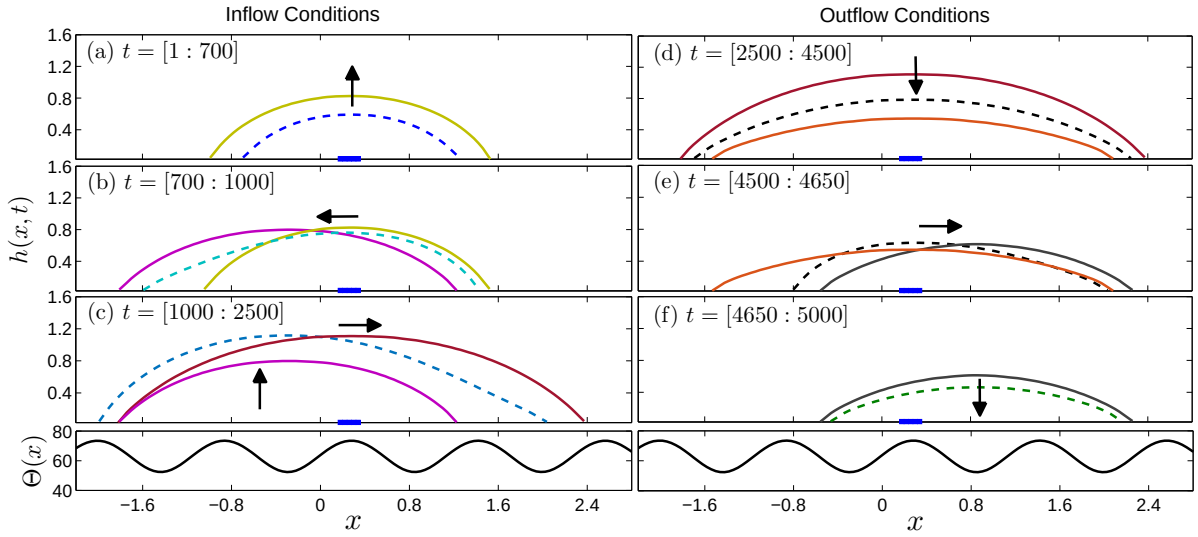

Figure 3: Numerical computations of a droplet with an inflow BC (a,b,c) and an outflow BC (d,e,f). The location of the small pore is marked as a blue rectangle which is placed at the center of the droplet. Arrows indicate direction of movement and the very bottom panels show the periodic variation of the chemical substrate. (a) Simulations start with an inflow BC and the volume increases (solid line). (b) As the volume increases the droplets shifts to the left, and (c) to the right again reaching the final state. (d) Simulation are stopped and start again with an outflow BC and so the volume decreases (dashed line). (e) As the volume decreases the droplet shifts to the right, and (f) remains in that new position.

3 COMPUTATIONAL RESULTS

We start by considering a droplet lying on top of a flat substrate with a periodic chemical heterogeneity as shown in Fig. 1. In particular we impose that the paramter A in Eq. (7) varies as $A = 0.3 + \sigma_0 \sin(\lambda_0 x)$ with $\sigma_0 = 0.1$. It can be shown that for this particular function of A, the corresponding equilibrium contact angle [cf. Eq. (7)] can be approximated by Eq. (1) with $\sigma = 10$, $\lambda = \lambda_0$, and $\theta_0 = 59°$. In our computations we consider two values for λ, namely $\lambda = 20$ and $\lambda = 100$ which gives rise to the two different substrates shown in Fig. 1. In addition, we impose an inflow BC until time t_f after which the BC is switched over to outflow conditions. Figure 2 shows the time-dependent variation of the volume where we can see that it increases and decreases linearly.

Figure 3 shows the dynamics of the droplet as the volume varies in time. As the volume increases the droplet remains centered at the same position (i.e. the displacement ℓ is not changing) until it reaches some critical volume for which the droplet suddenly shifts to the left [cf. Fig. 3(b)]. During this movement, one of the two contact points exhibits a stick-slip motion while the other one remains nearly at the same position. As we keep increasing the volume the droplet remains at this position for some range of volumes until it shifts back to the right, returning hence to the initial position [cf. Fig. 3(c)]. At this point, the simulations start again with an outflow BC and the droplet volume decreases while it remains at the same position [cf. Fig. 3(d)]. For a critical value of the volume we observe that the droplet shifts now to the right [cf. Fig. 3(e)] and remains there as the volume keeps decreasing [cf. Fig. 3(f)].

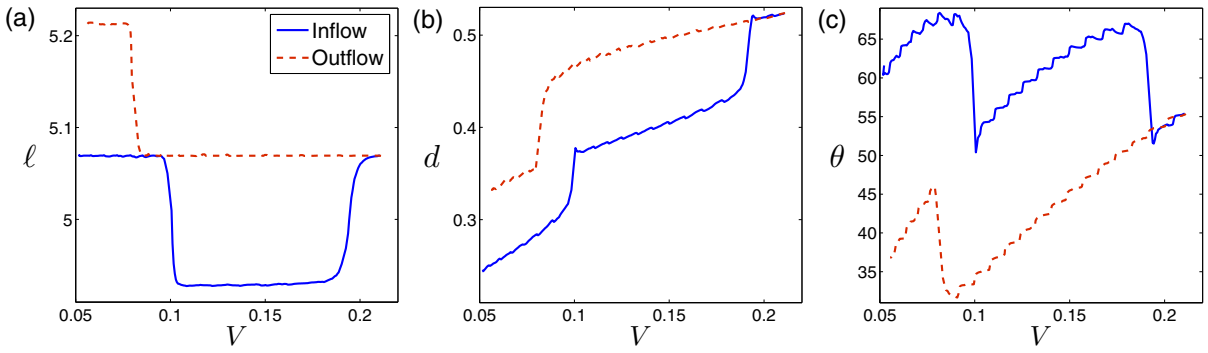

Figure 4: Numerical computations of a the different quantities characterizing the droplet dynamics as the volume is increased and decreased: displacement ℓ (a), droplet base d (b), and one of the contact angles θ (c). The wavelength of the chemical heterogeneity is $\lambda = 20$.

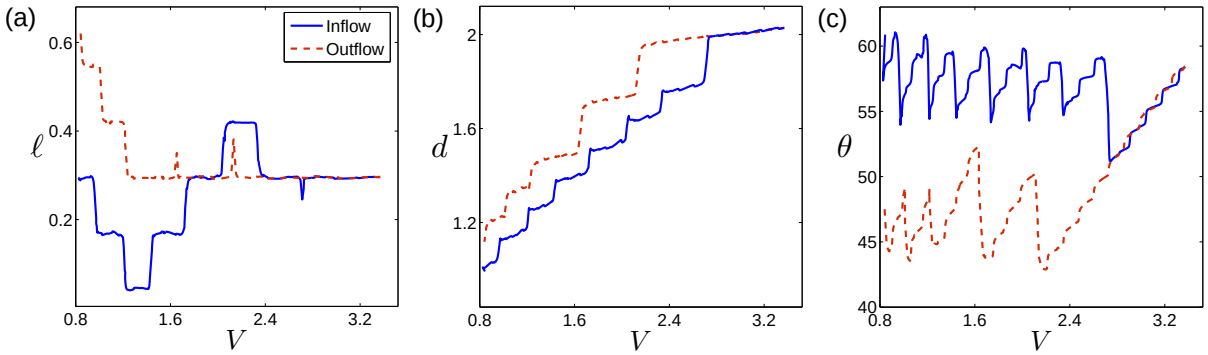

Figure 5: Numerical computations of a the different quantities characterizing the droplet dynamics as the volume is increased and decreased: displacement ℓ (a), droplet base d (b), and one of the contact angles θ (c). The wavelength of the chemical heterogeneity is $\lambda = 100$.

To quantify the droplet dynamics, we monitor the droplet displacement ℓ, the base d and one of the contact angles, namely $\theta = \theta_1$. Figure 4 shows all numerical results. We observe that the displacement ℓ exhibits a clear hysteresis loop as the volume is increased and decreased which is induced by the chemical heterogeneity. Similarly, the droplet base and the contact angle exhibit a similar behaviour characterised by stick-slip motion and hysteresis. Interestingly, if we increase the wavelength of the chemical heterogeneity (see Fig. 5 for numerical results by using $\lambda = 100$), such stick-slip motion becomes more prominent as the volume is increased/decreased. Consequently, the paths followed by the droplet as the volume is increased/decreased appear to be completely different, particularly for the displacement ℓ [cf. Fig. 5(a)].

4 CONCLUSIONS

We have presented computational evidence that a chemically modified substrate plays a crucial role on the dynamics of a droplet with a time-dependent volume. Our computational framework is based on a diffuse-interface model that incorporates an inflow/outflow boundary condition which we impose as an additional condition for the chemical potential. Our model is expected to be valid in a quasi-static regime, where the dynamics is dominated by diffusion-like mechanisms.

By imposing a simple periodic variation in the chemical properties of the substrate, we have observed that the dynamics of the droplet is charaterized by very rich phenomena, in terms of hysteresis behaviour and a stick-slip motion of the contact points as the volume is increased. In particular, all the quantities which characterize the droplet, namely its displacement, droplet base, and contact angle, undergo a hysteresis loop as the volume varies, indicating that the droplet follows different paths depending on whether the volume increases or decreases in time. In addition, our results have shown that such complex behaviour becomes more prominent as the wavelength of the periodic chemical variation is increased.

Finally, there is a number of interesting questions motivated by this preliminary study. For example, it would be interesting to consider droplets with a dynamic volume variation over not only periodic substrates but also more complex geometries, e.g. considering a chemical and/or topographical disorder. We shall address these and related issues in future studies.

Acknowledgments
This work is supported by the European Research Council through Advanced Grant No. 247031.

References

[1] D.M. Anderson, G.B. McFadden, and A.A. Wheeler. Diffuse-interface methods in fluid mechanics. *Annu. Rev. Fluid Mech.*, 30:139, 1998.

[2] C. Aydemir. Time-dependent behavior of a sessile water droplet on various papers. *Int. J. Polym. Mater.*, 59:387–397, 2010.

[3] S. Brandon, N. Haimovich, E. Yeger, and A. Marmur. Partial wetting of chemically patterned surfaces: The effect of drop size. *J. Colloid Interface Sci.*, 263:237–243, 2003.

[4] A.J. Briant, P. Papatzacos, and J. M. Yeomans. Lattice boltzamn simulations of contact line motion in a liquid-gas system. *Phil. Trans. Roy. Soc. Lond. A*, 360(1792):485–495, 2002.

[5] J. W. Cahn. Critical point wetting. *J. Chem. Phys.*, 66:3667, 1977.

[6] M.J. Cheah, I.G. Kevrekidis, and J. Bezinger. Water slug formation and motion in gas flow channels: The effects of geometry, surface wettability, and gravity. *Langmuir*, 29:9918–9934, 2013.

[7] C.E. Colosqui, M.J. Cheah, I.G. Kevrekidis, and J. Bezinger. Droplet and slug formation in polymer electrolyte membrane fuel cell flow channels: The role of interfacial forces. *J. Power Sources*, 196:10057–10068, 2011.

[8] P. G. de Gennes. Wetting: statics and dynamics. *Rev. Mod. Phys.*, 57:827–863, 1985.

[9] J. Drelich, J. D. Miller, and R. J. Good. The effect of drop (bubble) size on advancing and receding contact angles for heterogeneous and rough solid surfaces as observed with sessile-drop and captive-bubble techniques. *J. Colloid Interface Sci.*, 179:37–50, 1996.

[10] C. W. Extrand. A thermodynamic model for contact angle hysteresis. *J. Colloid Interface Sci.*, 207:11–19, 1998.

[11] E. Gauthier, T. Hellstern, I.G. Kevrekidis, and J. Bezinger. Drop detachment and motion on fuel cell electrode materials. *ACS Appl. Mater. Interfaces*, 4:761–771, 2012.

[12] A. Hennig, K. J. Eichhorn, U. Staudinger, K. Sahre, M. Rogalli, M. Stamm, A. W. Neumann, and K. Grundke. Contact angle hysteresis: study by dynamic cycling contact angle measurements and variable angle spectroscopic ellipsometry on polyimide. *Langmuir*, 20:6685–6691, 2004.

[13] P.C. Hohenberg and B.I. Halperin. Theory of dynamic critical phenomena. *Rev. Mod. Phys.*, 49:435–479, 1977.

[14] J. J. Huang, C. Shu, and Y. T. Chew. Lattice Boltzmann study of droplet motion inside a grooved channel. *Phys. Fluids*, 21:022103, 2009.

[15] D. Jacqmin. Contact-line dynamics of a diffuse fluid interface. *J. Fluid Mech.*, 402:57, 2000.

[16] R. Ledesma-Aguilar, D. Vella, and J. M. Yeomans. Lattice-boltzmann simulations of droplet evaporation. *Soft Matter*, 10:8267–8275, 2014.

[17] A. Marmur. Contact angle hysteresis on heterogeneous smooth surfaces. *J. Colloid Interface Sci.*, 168:40–46, 1994.

[18] P. Papatzacos. Macroscopic two-phase flow in porous media assuming the diffuse-interface model at pore level. *Transport Porous Med.*, 49(2):139–174, 2002.

[19] M. Queralt-Martín, M. Pradas, R. Rodríguez-Trujillo, M. Arundell, E. Corvera-Poiré, and A. Hernández-Machado. Pinning and avalanches in hydrophobic microchannels. *Phys. Rev. Lett.*, 106:194501, 2011.

[20] N. Savva, S. Kalliadasis, and G. P. Pavliotis. Two-dimensional droplet spreading over random topographical substrates. *Phys. Rev. Lett.*, 104:084501, 2010.

[21] N. Savva, G. P. Pavliotis, and S. Kalliadasis. Contact lines over random topographical substrates. Part 1. Statics. *J. Fluid Mech.*, 672:358, 2011.

[22] N. Savva, G. P. Pavliotis, and S. Kalliadasis. Contact lines over random topographical substrates. Part 2. Dynamics. *J. Fluid Mech.*, 672:384, 2011.

[23] P. Seppecher. Moving contact lines in the Cahn-Hilliard theory. *Int. J. Eng. Sci.*, 34:977, 1996.

[24] DN Sibley, A Nold, N Savva, and S Kalliadasis. The contact line behaviour of solid-liquid-gas diffuse-interface models. *Phys. Fluids*, 25, 2013.

[25] DN Sibley, A Nold, N Savva, and S Kalliadasis. On the moving contact line singularity: Asymptotics of a diffuse-interface model. *Eur. Phys. J. E*, 36, 2013.

[26] C. Wylock, M. Pradas, B. Haut, P. Colinet, and S. Kalliadasis. Disorder-induced hysteresis and nonlocality of contact line motion in chemically heterogeneous microchannels. *Phys. Fluids*, 24:032108, 2012.

[27] P. Yue, C. Zhou, and J.J. Feng. Sharp-interface limit of the Cahn-Hilliard model for moving contact lines. *J. Fluid Mech.*, 645:279, 2010.